# INVESTIGATION OF HIGH REPETITION RATE FEMTOSECOND ELECTRON DIFFRACTION AT PITZ

H. Qian[#], M. Gross, M. Krasilnikov, A. Oppelt, F. Stephan, DESY, Zeuthen, Germany

*Abstract*

PITZ is a photoinjector test facility for FLASH and European XFEL, and it has been proposed to be a prototype machine to develop an accelerator based THz/IR source for European XFEL pump-probe experiment. In addition, the machine can also support femtosecond electron diffraction at the same beam repetition rate as European XFEL, which brings XFEL users more flexibility for different experiments. In this paper, a femtosecond electron diffraction scheme based on the PITZ accelerator setup is investigated.

## INTRODUCTION

With the advances in ultra-bright electron and X-ray sources, it is now possible to observe ultrafast dynamics at the atomic level, with sub-Å spatial resolution and sub-~100 fs temporal resolution, either by femtosecond electron or femtosecond X-ray pump-probe experiments. Compared with X-ray diffraction, femtosecond electron diffraction has better transverse resolution due to shorter wavelength (~0.01 Å) and ~$10^5$ higher scattering cross section which is better for thin (sub-µm) or dilutes samples, but much weaker transverse coherence and peak brightness than X-ray FEL. Electron and X-ray are complementary tools for users to look at different samples or parameter spaces.

Traditionally, most electron scattering instruments operate in the 10-300 keV range, and due to space charge effects, such electron sources are limited to single electron or few electrons per bunch operation when both high transverse coherence and sub-100 fs resolution are required. Besides, velocity of 10-300 keV beam (0.19-0.77 c) is much slower than speed of light, so there is a velocity mismatch between electron probe and pump laser when traversing the sample, limiting time resolution to be above 100 fs (FWHM) for thick samples (~100 µm), such as gas phase experiments [1].

In the last decade or so, ultrafast electron diffraction (UED) and microscopy instruments benefit from the peak brightness of MeV electron sources developed for free electron lasers [2-6]. Single shot electron diffraction with sub-100 fs (rms) bunch length and relative transverse coherence of $10^{-5}$ becomes possible. In addition, the beam velocity is almost speed of light (0.99 c), so the velocity mismatch in gas phase experiments is mitigated.

Photoinjector test beamlines usually consist of a photocathode RF gun, a booster linac and diagnostics, which can be easily transformed into an ultrafast electron diffraction beamline. In this paper, PITZ is used as an example to show beam optimization for ultrafast electron

#houjun.qian@desy.de

diffraction applications based on the existing beamline layout.

## PITZ BEAMLINE FOR UED APPLICATIONS

PITZ is a photoinjector test facility, as shown in Fig. 1. The core of the facility is a high gradient (~60 MV/m) L-band normal conducting photocathode RF gun with long RF pulse width (~650 µs) operating at 10 Hz [7]. Due to the long RF pulse length, the high acceleration gradient and advanced photocathode laser system, PITZ gun provides MHz rate high brightness bunch train operation, which supports FEL operation at FLASH and XFEL. Besides the gun, the PITZ beamline also includes a normal conducting booster linac which is also capable of ~200 µs RF pulse operation at ~18 MV/m. With reduced gradient requirements for UED applications, both gun and booster linac can extend their RF pulse length to ~ 1 ms at 10 Hz operation, enabling higher electron flux for such applications.
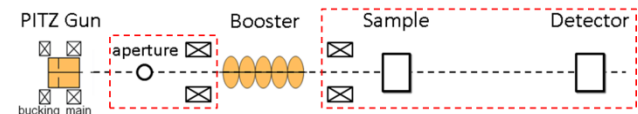


Figure 1: PITZ beamline optimization for UED applications (elements in red boxes are not present in the current PITZ beamline).

Compared to FEL applications, beam parameters for UED applications are quite different, as shown in Table 1. Due to low bunch charge for UED, beam emittance is dominated by thermal emittance, which is determined by the laser spot size on the cathode and the mean transverse momentum during photoemission. In order to further reduce beam emittance and dark current impact, a beam aperture is usually added, as shown in Fig. 1. If the aperture cut is in transverse momentum space instead of real space, another focusing element, e.g. a solenoid, is required to refocus the beam into the linac.

Table 1: Injector Beam Parameters for FEL and UED

|  | Charge | emittance | Bunch length |
| --- | --- | --- | --- |
| FEL | < 1 nC | < 1 µm.rad | ~10 ps |
| UED | < 1 pC | < 0.1 µm.rad | ~100 fs |

There are two ways to reach ~100 fs bunch length in photoinjectors for UED. One is direct generation at photocathode by ~100 fs laser, and the other is bunch compression in a drift space following a buncher cavity. In the second scheme, the photocathode laser can be longer than in the first scheme and transverse beam

brightness can be improved. At PITZ and other photoinjector facilities with a booster linac, the linac can be used as a buncher instead of an energy booster by changing the linac phase from on crest phase to zero crossing phase.

Besides the emittance compensation solenoid, another focusing element, e.g. solenoid or quadrupole, is located after the buncher to focus the beam on the sample and a detector for electron diffraction. A sample manipulation station is needed for pump-probe experiments, where interaction between electron beam, pump beam and sample happens. Downstream the sample station, a high efficiency detector is needed to record an electron diffraction pattern, consisting of a high efficiency electron scintillator screen and sensitive CCD cameras.

Compared with beam measurements for FEL applications, beam diagnostics for UED features femtocoulomb sensitivity and sub-100 fs resolution, e.g. beam profile screens, charge measurements, sub-100 fs bunch length measurements and beam arrival monitors.

## BEAM OPTIMIZATION FOR UED

The electron wavelength can be calculated by Eq. (1),

$$\lambda = \frac{h}{\gamma \beta m c} = \frac{\lambda_c}{\gamma \beta} . \qquad (1)$$

where $\lambda_c$ is Compoton wavelength, ~2.4 pm, $\gamma$ and $\beta$ are Lorentz factor and electron speed normalized by speed of light in vacuum, $h$ is Plank constant, $m$ is rest electron mass, $c$ is speed of light in vacuum. The diffraction limit at such a wavelength is $\lambda/_{4\pi}$, so the relative transverse coherence of the electron beam is

$$C_\perp = \frac{\lambda/4\pi}{\varepsilon_n/\gamma\beta} = \frac{\lambda_c/4\pi}{\varepsilon_n} \approx \frac{0.2 \ pm.rad}{\varepsilon_n} . \qquad (2)$$

i.e. the ratio of the phase space area between fully coherent radiation and electron beam, here $\varepsilon_n$ is the normalized transverse projected emittance. The coherence length of the electron beam can be calculated as

$$L_c = \frac{\lambda}{2\pi\sigma_\theta} = \frac{1}{\delta s} = 2\sigma_x C_\perp . \qquad (3)$$

where $\sigma_x$ and $\sigma_\theta$ are rms beam size and uncorrelated rms beam divergence, $\delta s$ is the rms resolution in reciprocal space of electron diffraction. The coherence length represents the upper limit of characteristic length over which the interference effect is still visible by the electron beam.

In state of the art MeV UED, $10^5 \sim 10^6$ electrons are needed for single shot electron diffraction on solid state samples with sub-100 fs bunch length and sub 20 nm.rad normalized emittance ($10^{-5}$ transverse coherence) [4, 8-9].

These parameters are achieved in simulation with the beamline shown in Fig. 1, see Table 2. Currently, PITZ photocathode laser is limited to a minimum pulse length of ~2 ps (FWHM) and a minimum spot size on cathode of ~200 μm, so both buncher and aperture cut are used in the simulations to enhance the temporal and spatial resolution of PITZ UED. Thermal emittance is assumed to be 0.5 μm.rad/mm in ASTRA simulation, which is available from both metal and semiconductor photocathodes [10].

Table 2: Simulations of Two UED Modes at PITZ

| Beam at sample | Single shot UED | Micro UED | Unit |
|---|---|---|---|
| Momentum | ~4 (<6.5) | ~4 (<6.5) | MeV/c |
| Wavelength | ~0.3 | ~0.3 | pm |
| Bunch FWHM length | <50 | <50 | fs |
| Pulse rate | ~$10^4$ | ~$10^4$ | pulse/s |
| Electron per pulse | ~$10^6$ | ~$10^3$ | e-/pulse |
| Normalized emittance | ~20 | ~0.2 | nm.rad |
| Relative coherence | ~$10^{-5}$ | ~$10^{-3}$ | |
| Beam rms size | ~100 | ~1 | μm |
| Coherence length | ~2 | ~2 | nm |
| Laser spot size at cathode | 200 | 2 | μm |

Sample conditions vary transversely, so local structure information probe on the sample with sub-μm electron beam size is very important. To achieve beam size reduction at the sample and to maintain the coherence length, beam emittance has to be reduced proportionally. Such an micro UED mode has been demonstrated at SLAC [11]. Besides, the micro UED is also good for reducing the thermal load at the sample for high repetition rate UED experiments, since the pump laser spot size can be reduced proportionally. Reducing beam emittance by aperture cuts the bunch charge quadratically. To reduce such a trend, beam emittance has to be improved from the cathode by either reducing the mean transverse momentum during photoemission or the photoemission spot size. In the simulation shown in Table 2, a 2 μm spot size is used for photoemission, a factor of 100 smaller than currently achievable at PITZ. According to beam brightness theory in the cigar beam regime [12], beam brightness is inversely proportional to the square root of photoemission spot size, so improvement of a factor of 10 is achieved for transverse brightness between the two modes in Table 2. In practice, the 2 μm photocathode laser spot size is very difficult to realize at PITZ. One idea is to create a special cathode where only the central area with 2 μm or smaller diameter is photoemitting.

## LIMITATION OF TEMPORAL RESOLUTION

UED based on RF guns benefits from both high acceleration gradient and relativistic beam energy for higher beam brightness, but suffers from RF jitter in both gun and buncher cavity. The RF jitter induces beam energy jitter and causes time of flight (TOF) jitter between cathode and sample. Even though electron beam can be bunched into sub-100 fs, MeV UED temporal resolution of sub-100 fs is still challenging due to relative timing jitter between pump beam and electron beam. The temporal resolution of UED pump probe experiment is calculated by [4, 6, 13]

$$\tau_{UED} = \sqrt{\tau_e^2 + \tau_{eTOA}^2 + \tau_{laser}^2 + \tau_{laserTOA}^2 + \tau_{VM}^2} \ . \quad (4)$$

where $\tau_e$ and $\tau_{laser}$ are electron beam bunch length and pump laser pulse duration, $\tau_{eTOA}$ and $\tau_{laserTOA}$ are time of arrival (TOA) jitter of electron beam and pump laser beam. For a beam energy of several MeV, the temporal resolution dilution $\tau_{VM}$ due to velocity mismatch between pump laser and electron beam inside the sample is negligible. Laser pulse length of tens of fs is commercially available, and electron beam bunch length of the similar order is also achievable in simulations although experimental demonstration and diagnostics are still challenging. Laser to RF synchronization in accelerator facility on the order of tens of fs has been achieved, although local realization at different accelerator facilities is still challenging. In state of the art MeV UED experiment, it's expected that the electron beam TOA jitter will dominate the temporal resolution. Different time stamping techniques have been proposed to post process the time sequence of UED patterns, but it's challenging for high repetition rate experiments. Due to limited frame rate of the detector, multiple diffraction patterns are integrated in one shot, in which timing jitter cannot be distinguished. In this case, beam TOA jitter has to be improved for better temporal resolution.
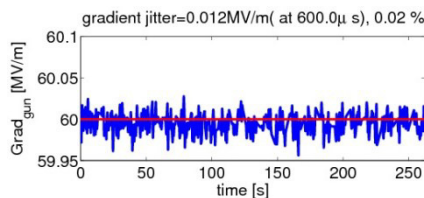


Figure 2: Gun RF amplitude jitter with feedback on.
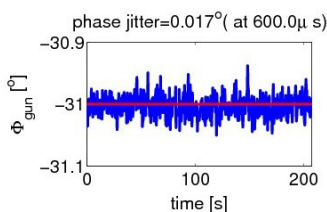


Figure 3: Booster RF phase jitter with feedback on.

In the PITZ case shown in Table 2, the gun phase is set to the maximum energy gain phase, and the buncher is set to the zero energy gain phase, so TOA is insensitive to both gun phase jitter and buncher amplitude jitter. For gun amplitude jitter, TOF jitter between gun and buncher will be suppressed by bunching process, and the final TOF jitter is defined by the distance between buncher and sample. Therefore the distance between buncher and sample should be minimized. Based on the current PITZ beamline setup, the distance between buncher and sample can be ~ 2 meters. For the buncher phase jitter, the TOF jitter is equivalent to $\delta\phi/\omega$, where $\delta\phi$ is the buncher phase jitter, and $\omega$ is the angular frequency of the buncher. In simulations of Table 2, the electron beam TOA jitter is

$$\tau_{eTOA} = \sqrt{\left(11fs \frac{\sigma_{\Delta A/A}^{gun}}{10^{-4}}\right)^2 + \left(21fs \frac{\sigma_{\Delta\phi}^{buncher}}{0.01^\circ}\right)^2} \ . \quad (5)$$

Fig. 2 and 3 show the RF jitter measured for the gun and buncher when feedback is on, and beam energy jitter measurement with gun only is also consistent with the ~2×10^-4 gun amplitude jitter. With the RF jitter shown in Fig. 2 and 3, the beam arrival jitter is about ~42 fs rms (~100 fs FWHM). Considering a state of the art laser system, ~100 fs (FWHM) time resolution is possible for UED at the PITZ beam line.

## CONCLUSION

In this paper, the PITZ beamline is optimized for UED applications by ASTRA simulations. It's shown PITZ can support both single-shot UED and micro-UED with ~100 fs (FWHM) temporal resolution. Both PITZ gun and linac support ~ 1 ms RF pulse length with gradients required by UED operation, which can enable $10^4$ pulses per second (MHz bunch train at 10 Hz repetition rate) for advanced UED experiments demanding higher electron flux.

## REFERENCES

[1] J. Yang *et al.*, Faraday Discuss., 194, 563-581 (2016).
[2] X. J. Wang, Z. Wu, and H. Ihee, in *Proc. PAC'03*, pp. 420.
[3] R. K. Li and P. Musumeci, Phys. Rev. Applied 2, 024003 (2014).
[4] S. P. Weathersby *et al.*, Rev. Sci. Instrum. 86, 073702 (2015).
[5] S. Manz *et al.*, Faraday Discuss., 2015, 177, 467 (2014).
[6] D. Filippetto and H Qian, J. Phys. B: At. Mol. Opt. Phys. 49 104003 (2016).
[7] M. Krasilnikov *et al.*, PRST AB 15, 100701 (2012).
[8] R. Li *et al.*, Journal of Applied Physics 110, 074512 (2011).
[9] M. Z. Mo *et al.*, Rev. Sci. Instrum. 87, 11D810 (2016).
[10] E. Prat *et al.*, PRST AB 18, 043401 (2015).
[11] X. Shen, R. Li and X. Wang, Microsc. Microanal. 22 (Suppl 3), 2016.
[12] D. Filippetto *et al.*, PRST AB 17, 024201 (2014).
[13] R. Li and C. Tang., Nucl. Instr. Meth., 605, 243 (2009).